Exciting dynamical behavior in a network of two coupled rings of Chen oscillators

Carla M. A. Pinto

Abstract We study exotic patterns appearing in a network of coupled Chen oscillators. Namely, we consider a network of two rings coupled through a "buffer" cell, with $\mathbf{Z}_3 \times \mathbf{Z}_5$ symmetry group. Numerical simulations of the network reveal steady states, rotating waves in one ring and quasiperiodic behavior in the other, and chaotic states in the two rings, to name a few. The different patterns seem to arise through a sequence of Hopf bifurcations, period-doubling, and halving-period bifurcations. The network architecture seems to explain certain observed features, such as equilibria and the rotating waves, whereas the properties of the chaotic oscillator may explain others, such as the quasiperiodic and chaotic states. We use XPPAUT and MATLAB to compute numerically the relevant states.

Keywords Chaos · Quasiperiodic states · Symmetry · Hopf bifurcation · Period-doubling bifurcation · Halving-period bifurcation

1 Introduction

In the last decade, a new theory concerning networks of coupled cells systems has been developed, mainly by Stewart et al. [32] and Golubitsky et al. [18]. Synchronized dynamical behavior and corresponding bifurcations have been particularly focused.

Coupled cell networks are known to exhibit rich patterns, like synchrony, phase-relations, quasiperiodic motion, synchronized chaos, among others [5,6,15,23,27]. The graphs architecture seems to have a great importance in the understanding of these phenomena; nevertheless, it seems to not be able to fully explain them.

Networks of coupled cells may arise as models of animal and robot locomotion, speciation, visual perception, electric power grids, internet communication, secure communication [7–11,20,21,24,26,28,30,31], and many others.

General coupled cell networks may be divided into two groups, namely coupled cells systems that possess some degree of symmetry and coupled cells systems with no symmetry. In the first group, one can find the networks with exact symmetry group.

In this paper, we study interesting dynamical features occurring in a coupled system of two unidirectional rings, coupled through a "buffer" cell, with $\mathbf{Z}_3 \times \mathbf{Z}_5$ exact symmetry. In Sect. 2, we provide a review of the coupled cells networks formalism and bifurcation theory. In Sect. 3, we simulate the coupled cells systems associated to the network of two coupled rings of cells in Fig. 1 and discuss the results. In Sect. 4, we conclude this work and shed some light on future research directions.

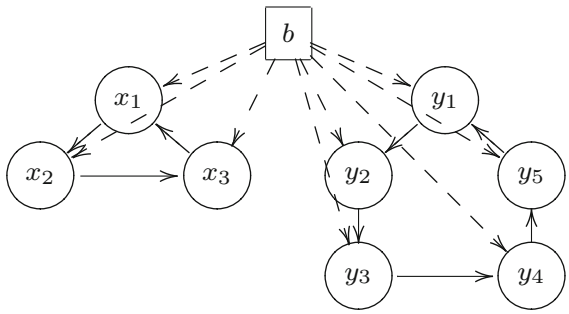

Fig. 1 Network of two coupled unidirectional rings, one with three cells and the other with five, connected through a "buffer" cell b. The network has $\mathbf{Z}_3 \times \mathbf{Z}_5$ symmetry group

2 Coupled cells and symmetry

Networks of coupled cells are usually represented schematically by a directed graph. The graphs' nodes correspond to individual cells and the edges to the couplings between them. A "cell" means a nonlinear dynamical system of ordinary differential equations.

Mathematically, a coupled cells system consists of a finite set of nodes (or cells) $\mathcal{C}$, and a finite set of edges $\mathcal{E}$. It is defined an equivalence relation on cells in $\mathcal{C}$, where the equivalence class of c is the type of cell c, and an input set of cells $\mathcal{I}(c)$, which consists of cells whose edges have cell c as head. Moreover, it is defined an equivalence relation on the edges (or arrows), where the equivalence class of e is the type of edge e, and it satisfies the condition that "equivalent edges have equivalent tails and edges." The last condition means that equivalent edges must have tails and edges of the same equivalence class.

For each cell, c is defined an internal phase space P_c. The total phase space of the network is the product $P = \prod_{i=1}^{n} P_c$. The coordinates on P_c are denoted by x_c, and the coordinates on P are thus $(x_1, x_2, \ldots, x_n)$. At time t, the system is at state $(x_1(t), x_2(t), \ldots, x_n(t))$.

A vector field f on P that is compatible with the network architecture is said to be *admissible* for that network, and satisfies two conditions: (1) the domain and (2) the pull-back condition. The domain condition imposes that each component f_i corresponding to cell c_i must be a function of the cells in the input set of cell c_i, $\mathcal{I}(c_i)$. The pull-back condition states that the components f_i and f_j of cells c_i and c_j are identical, up to a suitable permutation of the relevant variables, if the two cells have isomorphic input cells [16].

A symmetry of a coupled cells system is the group of permutations of the cells (and arrows) that preserve the network structure (including cell types and arrow types), and its action on P is by permutation of cell coordinates. It is thus a transformation of the phase space that sends solutions to solutions. The network in Fig. 1 is an example of a network with $\mathbf{Z}_3 \times \mathbf{Z}_5$ symmetry. This means that we can permute all cells in each ring.

2.1 Bifurcations

The study of the local bifurcations in symmetric (equivariant) coupled cells systems is done in [17, 19]. The existence of certain branches of symmetry-breaking steady states is proven by a local bifurcation theorem, the Equivariant Branching Lemma [19]. The Equivariant Hopf Theorem guarantees the existence of families of small-amplitude periodic solutions bifurcating from the origin [19]. Another way of obtaining periodic solutions in an equivariant system is the H mod K theorem [9,17]. For a finite symmetry group Γ, this theorem gives necessary and sufficient conditions for the existence of a equivariant system of ODEs and a periodic solution $x(t)$ to that system with specified spatiotemporal symmetries.

Let Γ be a finite group of symmetries of the following systems of ODEs:

$$\frac{\mathrm{d}x}{\mathrm{d}t} = f(x). \tag{1}$$

Let $x(t)$ be a periodic solution of system 1, with period normalized to 1, and let $\gamma \in \Gamma$. By symmetry, we know that $\gamma x(t)$ is also a solution to (1). We consider two cases, either both solutions intersect (thus, are identical) or the two trajectories do not intersect.

Consider that both solutions are identical, and then by uniqueness of solutions, there is $\theta \in \mathbf{S}^1$ such that

$$\gamma x(t) = x(t-\theta) \quad \text{or} \quad \gamma x(t+\theta) = x(t),$$

and we say that $x(t)$ has spatiotemporal symmetry $\gamma \in \Gamma$, where θ is the temporal phase shift that corresponds to γ. If $\theta = 0$, then γ is a spatial symmetry.

Define K to be the subgroup of all spatial symmetries and H to be the subgroup of all spatiotemporal symmetries. Mathematically, we have

$$\begin{aligned} K &= \{\gamma \in \Gamma : \gamma x(t) = x(t) \text{ for all } t\} \\ H &= \{\gamma \in \Gamma : \gamma\{x(t)\} = \{x(t)\} \text{ for all } t\}. \end{aligned} \tag{2}$$

Filipski and Golubitsky [14] enumerate the symmetries of periodic solutions obtained from Hopf bifurcation in coupled cell systems with finite abelian symmetries. Moreover, they classify the spatiotemporal periodic solutions of coupled systems with $\mathbf{Z}_l \times \mathbf{Z}_k$ symmetry, which are obtainable by a generic Hopf bifurcation, and show that there are families of spatiotemporal periodic solutions that cannot be obtained by this type of bifurcation.

We can list all spatiotemporal periodic states that are expected to occur when the coupled cell systems associated to the network of Fig. 1 undergoes a symmetry-breaking Hopf bifurcation (primary Hopf bifurcation). There are two types of solutions: one with $\tilde{\mathbf{Z}}_3 \times \mathbf{Z}_5$ symmetry and another with $\mathbf{Z}_3 \times \tilde{\mathbf{Z}}_5$. These solutions corresponding to these subgroups are also called *rotating waves*.

The form of these periodic solutions is described as follows. The periodic solution of type $\tilde{\mathbf{Z}}_3 \times \mathbf{Z}_5$ is such that its components corresponding to the cells in the 3-ring are periodic and have the same wave form, but they are $1/3$ out of phase and the components corresponding to the cells in the 5-ring stay in equilibrium. Similarly, the periodic solution of type $\mathbf{Z}_3 \times \tilde{\mathbf{Z}}_5$ is such that its components corresponding to the cells in the 5-ring are periodic and have the same wave form, but they are $1/5$ out of phase, and the components corresponding to the cells in the 3-ring stay in equilibrium.

3 Numerical simulations

The coupled cells system, associated with the network depicted in Fig. 1, is simulated. We use XPPAUT [13] and MATLAB [34] to compute numerically the relevant states. We consider the Chen oscillator as the phase space for each cell of the two rings and an unidimensional phase space for the "buffer cell." The total phase space is thus twenty-fifth dimensional. The dynamics of a singular ring cell is given by [12,25]

$$\begin{aligned} \dot{u} &= a(v-u) \\ \dot{v} &= (c-a)u - uw + cv \\ \dot{w} &= uv - bw, \end{aligned} \tag{3}$$

where a, b, and c are real parameters.

The unidimensional dynamics of the "buffer cell" is given by [3,15]

$$f(u) = \mu u - \frac{1}{10}u^2 - u^3, \tag{4}$$

where $\mu = -1.0$ is a real parameter.

The coupled cells system of equations associated to the network in Fig. 1 is given by

$$\begin{aligned} \dot{x_j} &= g(x_j) + k\,(x_j - x_{j+1}) + d\,b \quad j = 1, \ldots, 3 \\ \dot{b} &= f(b) \\ \dot{y_j} &= g(y_j) + k\,(y_j - y_{j+1}) + d\,b \quad j = 1, \ldots, 5, \end{aligned} \tag{5}$$

where $g(u)$ represents the dynamics of each Chen oscillator $a = 35$, $b = 3$, $k = -5.0$, $d = 0.2$, and the indexing assumes $x_4 \equiv x_1$ and $y_6 \equiv y_1$. We assume that the coupling between all cells is linear and is done only in the first variable of each Chen oscillator.

We vary parameter $c \in [15, 28]$, going from lower to higher values, and start from a steady state of the whole system.

In Fig. 2, we plot (top) the time series solution of the coupled cell system (5), and (bottom) we represent the phase plane of oscillator y_1 of the 5-ring. The solution is a rotating wave state in the 5-ring, obtained by a Hopf bifurcation (HB1), from the trivial equilibrium branch. Cells in the 3-ring are at equilibrium. These solutions can be explained using the Equivariant Hopf Theorem for coupled cell systems in the symmetric case [19]. The bifurcation has occured in the 5-ring.

We increase c again, and another Hopf bifurcation occurs (HB2). In Fig. 3, we plot (top) the time series solution of the coupled cell system (5), and (center) we show the phase planes for the oscillator x_1 of the 3-ring (center, left) and for the oscillator y_1 of the 5-ring (center, right). The solution is a $\mathbf{Z}_3$ rotating wave in the 3-ring and a $\mathbf{Z}_5$ rotating wave in the other ring. The full solution is quasiperiodic (Fig. 3, bottom).

Figure 4 shows the time series further away from the tertiary Hopf bifurcation (HB3) in the coupled cell system (5). Unlike the previous cases (Figs. 2, 3), the amplitude of the solution is higher and the wave form is qualitatively different, displaying typical relaxation oscillatory features. Relaxation oscillations are solutions characterized by long periods of quasi-static behavior interspersed with short periods of rapid transition. These solutions are studied in the context of the canard phenomenon [22,33] in fast–slow systems.

After the third Hopf bifurcation point, a sequence of four Hopf bifurcations (HB4, HB5, HB6, and HB7) is observed for increasing values of c. As we move further and further away from (HB3), the qualitative behavior of the cells in the two rings becomes more complex, in the sense that becomes quasiperiodic and, after some value, turns chaotic (see Figs. 5, 6, 7, 8). This phenomenon suggests a period-doubling bifurcation phenom-

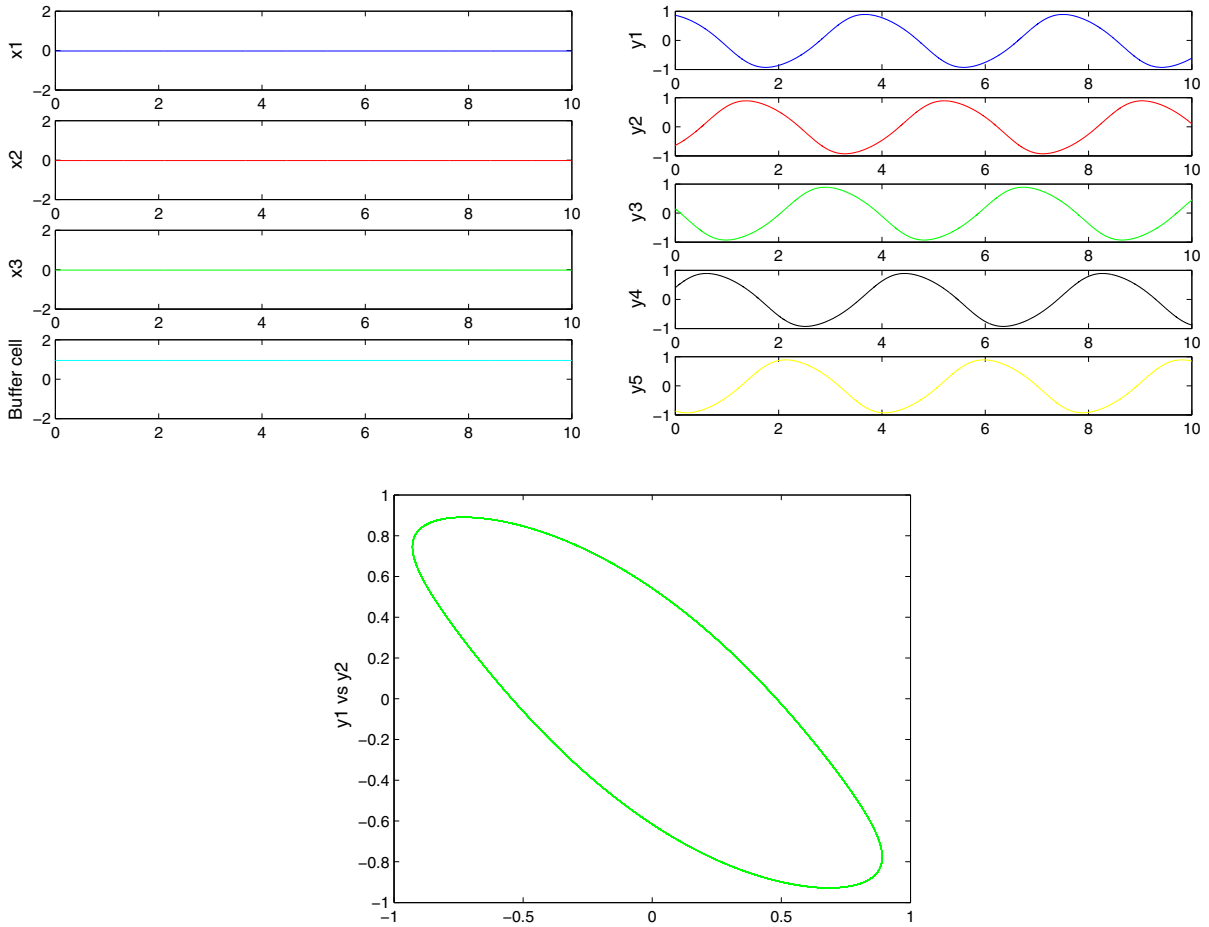

Fig. 2 Simulation of the coupled system (5) with $\mathbf{Z}_3 \times \mathbf{Z}_5$ symmetry. Time series from the nine cells after the first Hopf bifurcation point (*HB1*). (*Top, left*) Cells in the 3-ring are at equilibrium, and cells in the 5-ring display a $\mathbf{Z}_5$ rotating wave (*top, right*). (*Bottom*) Phase plane of oscillator y_1 of the 5-ring

ena leading to chaos. The existence of Chen's chaotic attractor is proved in [1].

Further away of the Hopf bifurcation point (HB7) and continuing increasing c, the qualitative behavior of the cells in the rings changes again. It seems as if the chaotic state is replaced by a quasiperiodic state. One may say that the chaotic "severity" is decreased (see Figs. 6, 7, 8, 9, 10). We believe that a sequence of halving-period bifurcations takes place, decreasing the period of the orbits, and after some value of c, we obtain again nice rotating waves in the two rings.

Thus, from the numerical results, we conclude that there is a richness of dynamic features produced by the network of two rings coupled through a "buffer" cell, with $\mathbf{Z}_3 \times \mathbf{Z}_5$ symmetry (Fig. 1). There are states where the cells in the first ring are at equilibrium and cells in the second ring show a rotating wave state, or even states where cells in the first ring show a quasiperiodic motion and cells in the second ring depict a rotating wave.

3.1 Discussion

Here, we describe the qualitative features of the bifurcation scenario represented in Fig. 11. This is a schematic bifurcation diagram of a sequence of seven Hopf bifurcations, where the first branch emanates from a trivial branch of steady states.

The solutions corresponding to the primary branch, which emanates from the trivial branch, at the first Hopf bifurcation point (HB1), represented in Fig. 11,

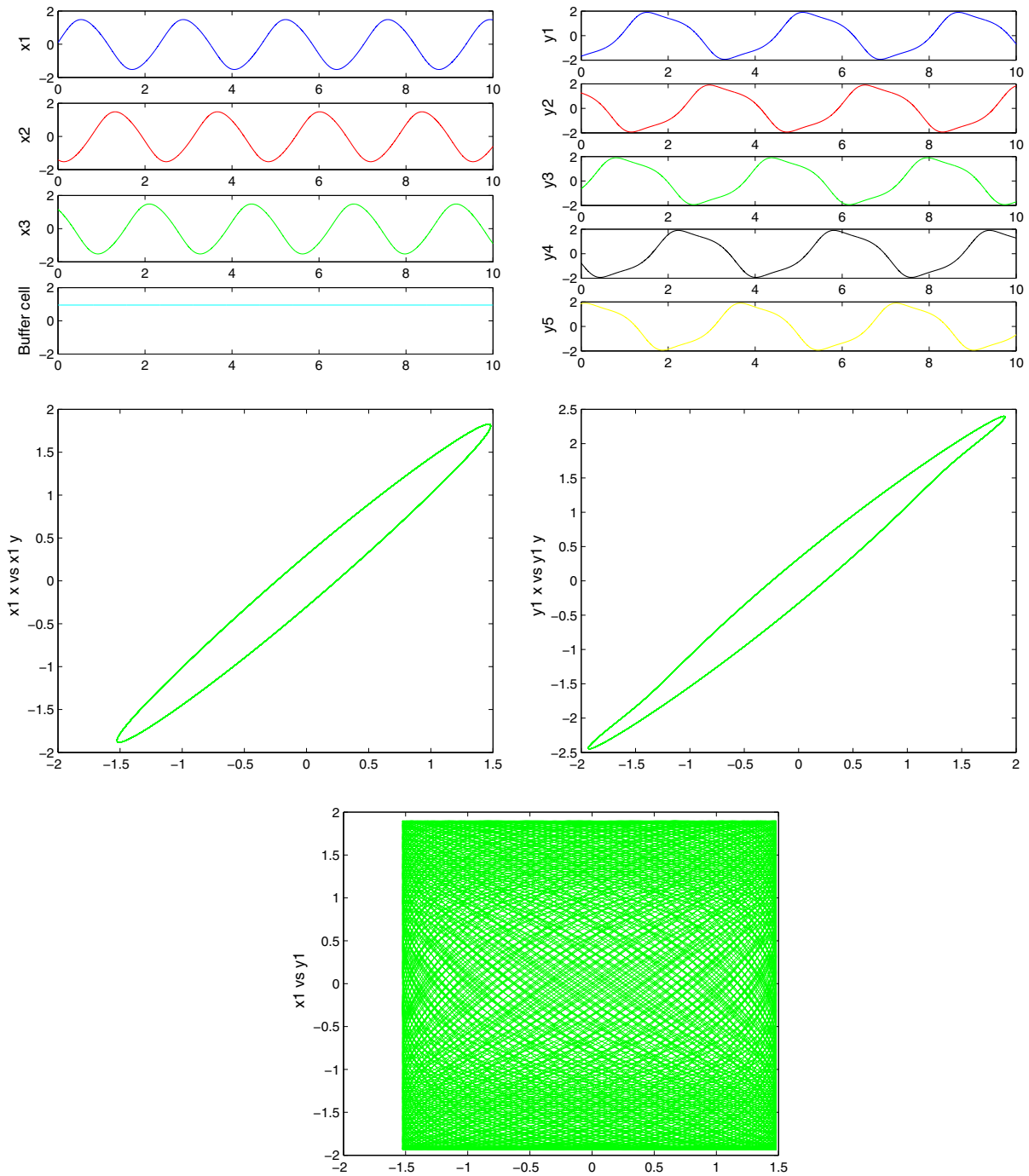

Fig. 3 Simulation of the coupled system (5) with $\mathbf{Z}_3 \times \mathbf{Z}_5$ symmetry, after the second Hopf bifurcation point (*HB2*). The cells in the 3-ring exhibit a $\mathbf{Z}_3$ rotating wave (*top, left*), and the cells in the other ring show a $\mathbf{Z}_5$ rotating wave (*top, right*). Phase planes of the oscillator x_1 (*center, left*) and of the oscillator y_1 (*center, right*). Cell x_1 vs cell y_1 (*bottom*). For more information, see text

can be explained using the Equivariant Hopf Theorem, for coupled cell systems in the symmetric case.

Since the symmetry group of the network in Fig. 1 is $\mathbf{Z}_3 \times \mathbf{Z}_5$; then, after the first Hopf bifurcation, we may obtain solutions with $\tilde{\mathbf{Z}}_3 \times \mathbf{Z}_5$ symmetry or with

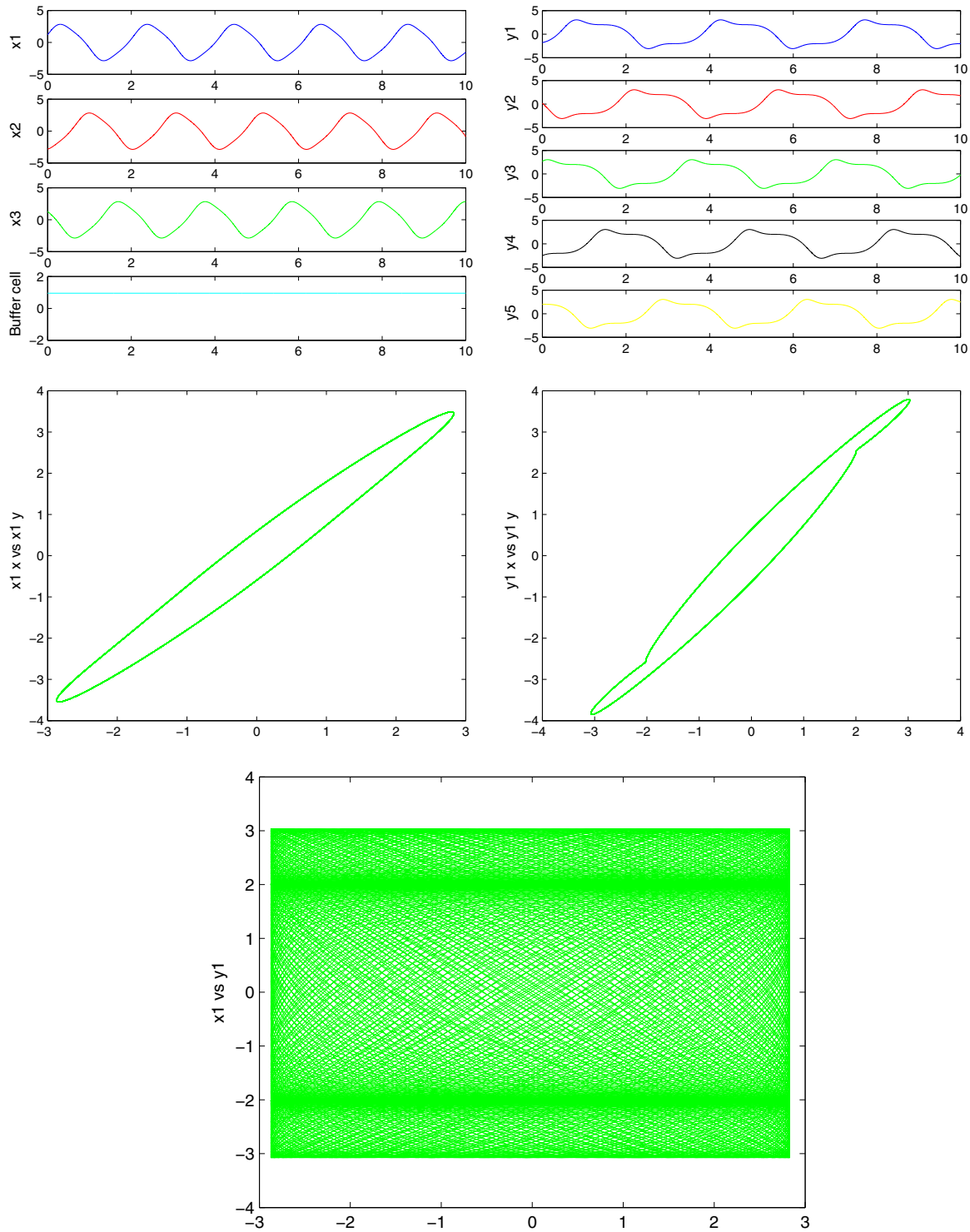

Fig. 4 Simulation of the coupled system (5) with $\mathbf{Z}_3 \times \mathbf{Z}_5$ symmetry, after the third Hopf bifurcation point (*HB3*). The cells in the 3-ring exhibit a $\mathbf{Z}_3$ rotating wave (*top, left*), whereas cells in the other ring depict a relaxation oscillation (*top, right*). Phase planes of the oscillator x_1 (*center, left*) and of the oscillator y_1 (*center, right*). Cell x_1 vs cell y_1 (*bottom*). For more information, see text

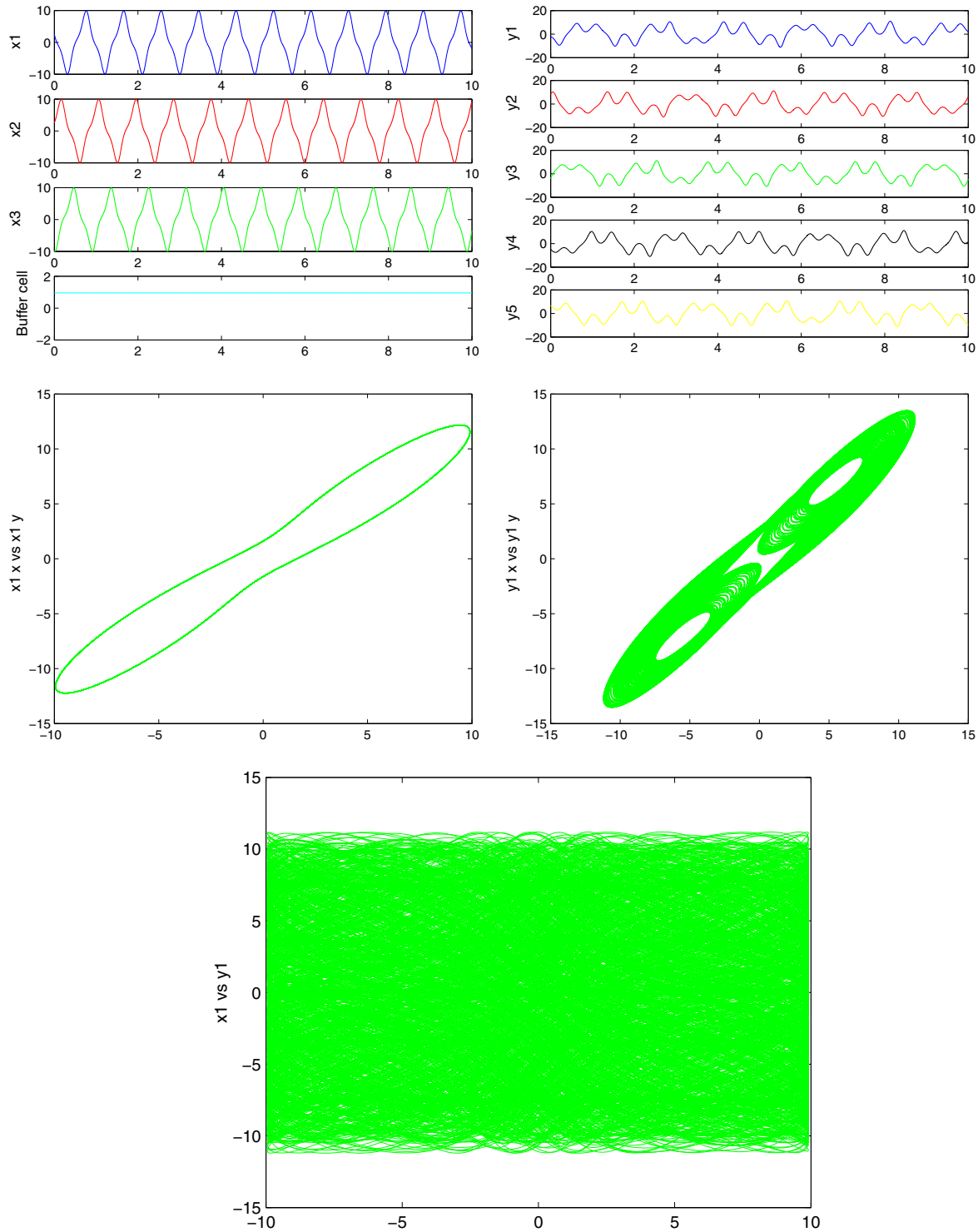

Fig. 5 Simulation of the coupled system (5) with $\mathbf{Z}_3 \times \mathbf{Z}_5$ symmetry, after the sixth Hopf bifurcation point (*HB6*). The cells in the 3-ring exhibit a $\mathbf{Z}_3$ rotating wave (*top, left*), whereas cells in the other ring depict a quasiperiodic solution (*top, right*). Phase planes of the oscillator x_1 (*center, left*) and of the oscillator y_1 (*center, right*). Cell x_1 vs cell y_1 (*bottom*). For more information, see text

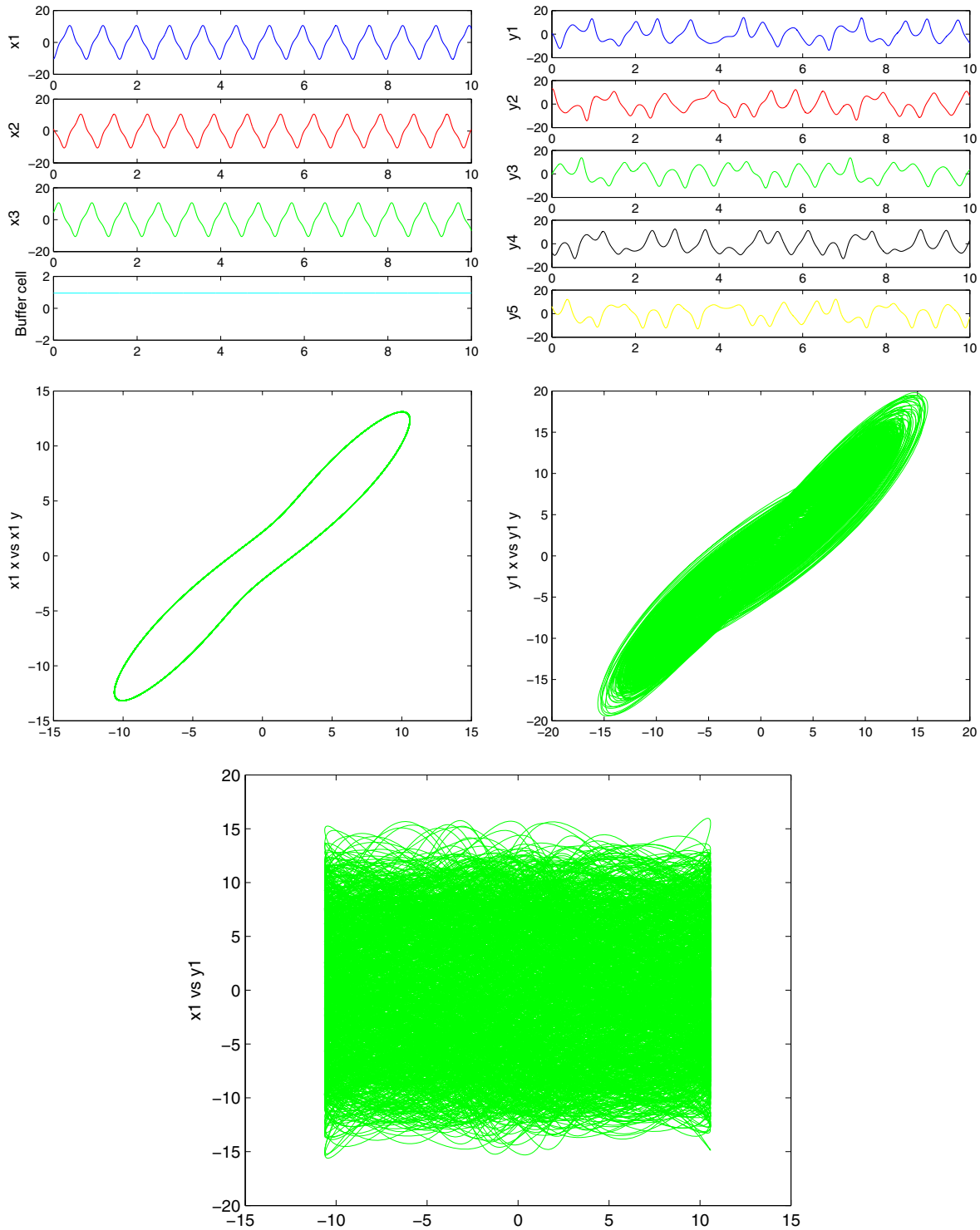

Fig. 6 Simulation of the coupled system (5) with $\mathbf{Z}_3 \times \mathbf{Z}_5$ symmetry, after the seventh Hopf bifurcation point (*HB7*). The cells in the 3-ring exhibit a $\mathbf{Z}_3$ rotating wave (*top, left*), whereas cells in the other ring depict a chaotic solution (*top, right*). Phase planes of the oscillator x_1 (*center, left*) and of the oscillator y_1 (*center, right*). Cell x_1 vs cell y_1 (*bottom*). For more information, see text

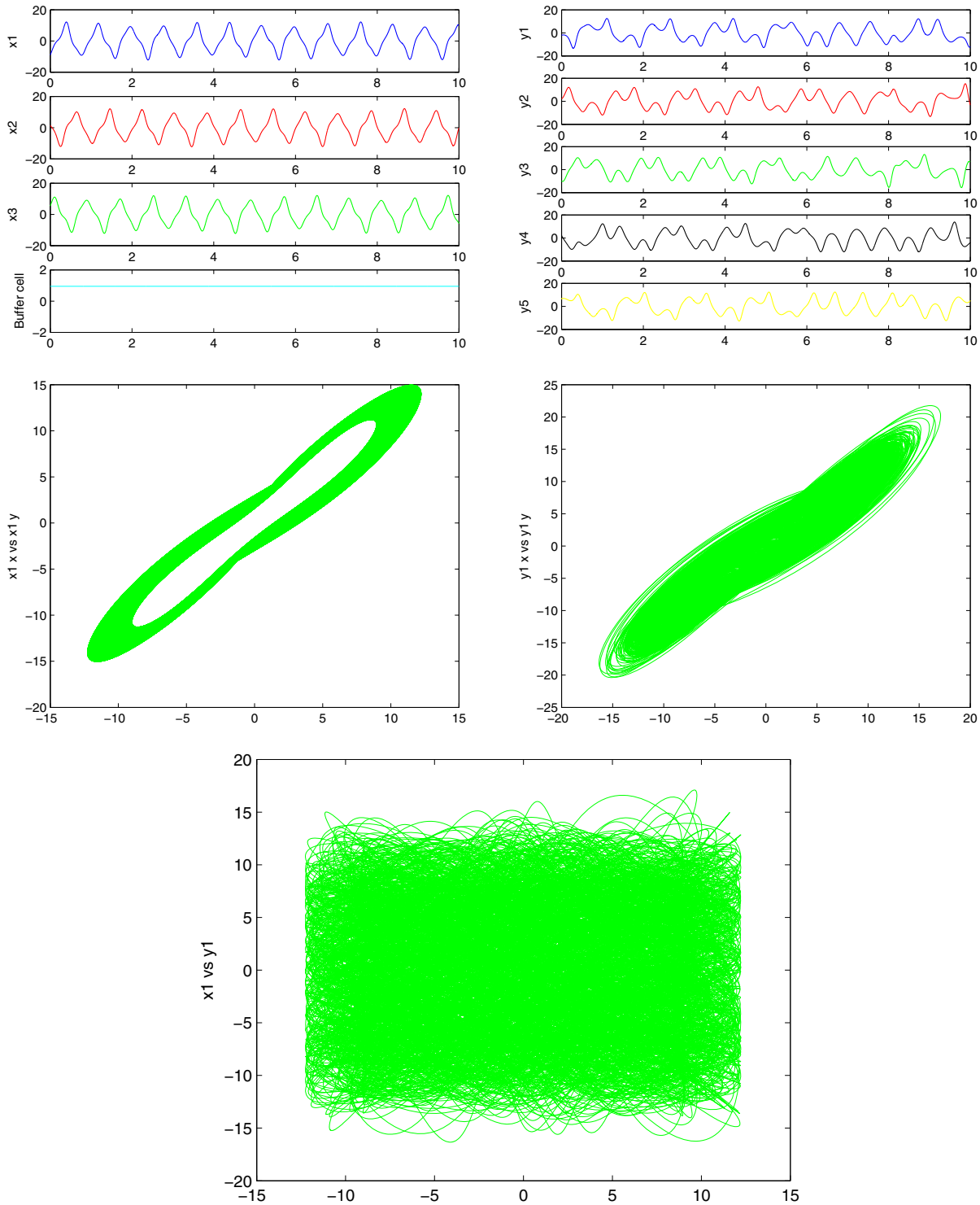

Fig. 7 Simulation of the coupled system (5) with $\mathbf{Z}_3 \times \mathbf{Z}_5$ symmetry, after the seventh Hopf bifurcation point (*HB7*). The cells in the 3-ring exhibit a quasiperiodic motion (*top, left*), whereas the cells in the other ring show a chaotic state (*top, right*). Phase planes of the oscillator x_1 (*center, left*) and of the oscillator y_1 (*center, right*). Cell x_1 vs cell y_1 (*bottom*). For more information, see text

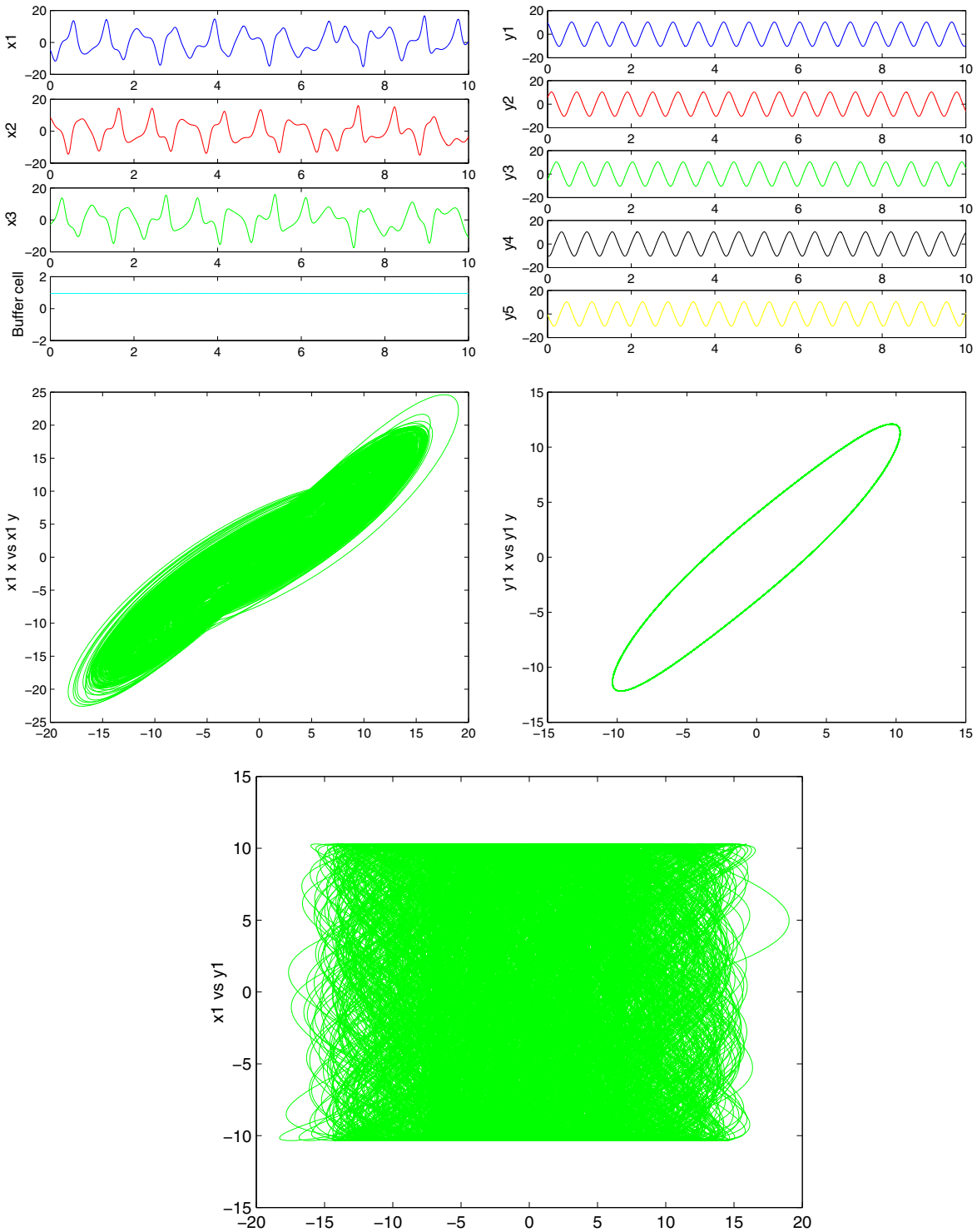

Fig. 8 Simulation of the coupled system (5) with $\mathbf{Z}_3 \times \mathbf{Z}_5$ symmetry, after the seventh Hopf bifurcation point (HB7). The cells in the 3-ring exhibit a chaotic motion (*top, left*), whereas the cells in the other ring show $\mathbf{Z}_5$ rotating wave (*top, right*). Phase planes of the oscillator x_1 (*center, left*) and of the oscillator y_1 (*center, right*). Cell x_1 vs cell y_1 (*bottom*). For more information, see text

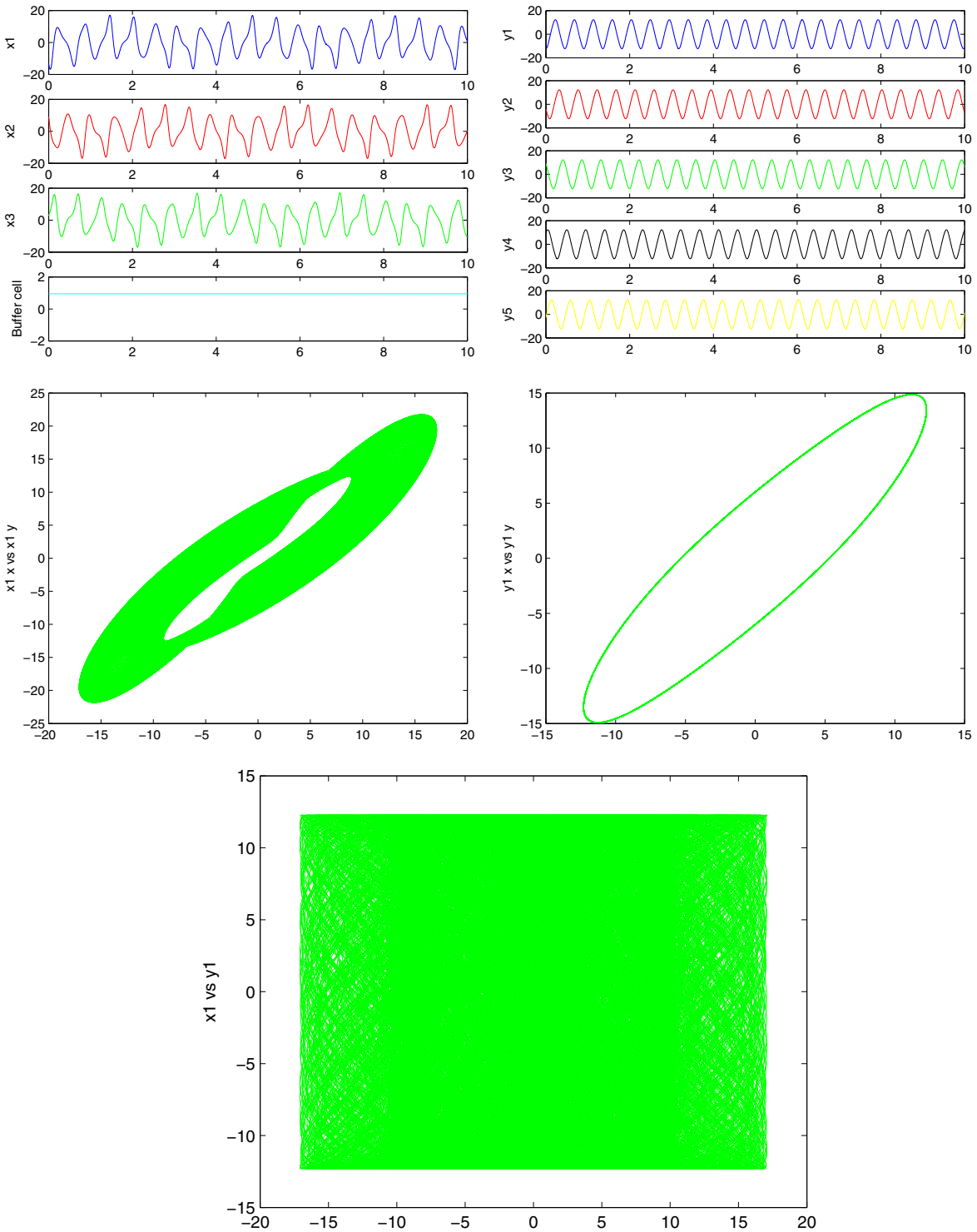

Fig. 9 Simulation of the coupled system (5) with $\mathbf{Z}_3 \times \mathbf{Z}_5$ symmetry, after the seventh Hopf bifurcation point (*HB7*). The cells in the 3-ring exhibit a quasiperiodic motion (*top, left*), whereas the cells in the other ring depict a rotating $\mathbf{Z}_5$ wave (*top, right*). Phase planes of the oscillator x_1 (*center, left*) and of the oscillator y_1 (*center, right*). Cell x_1 vs cell y_1 (*bottom*). For more information, see text

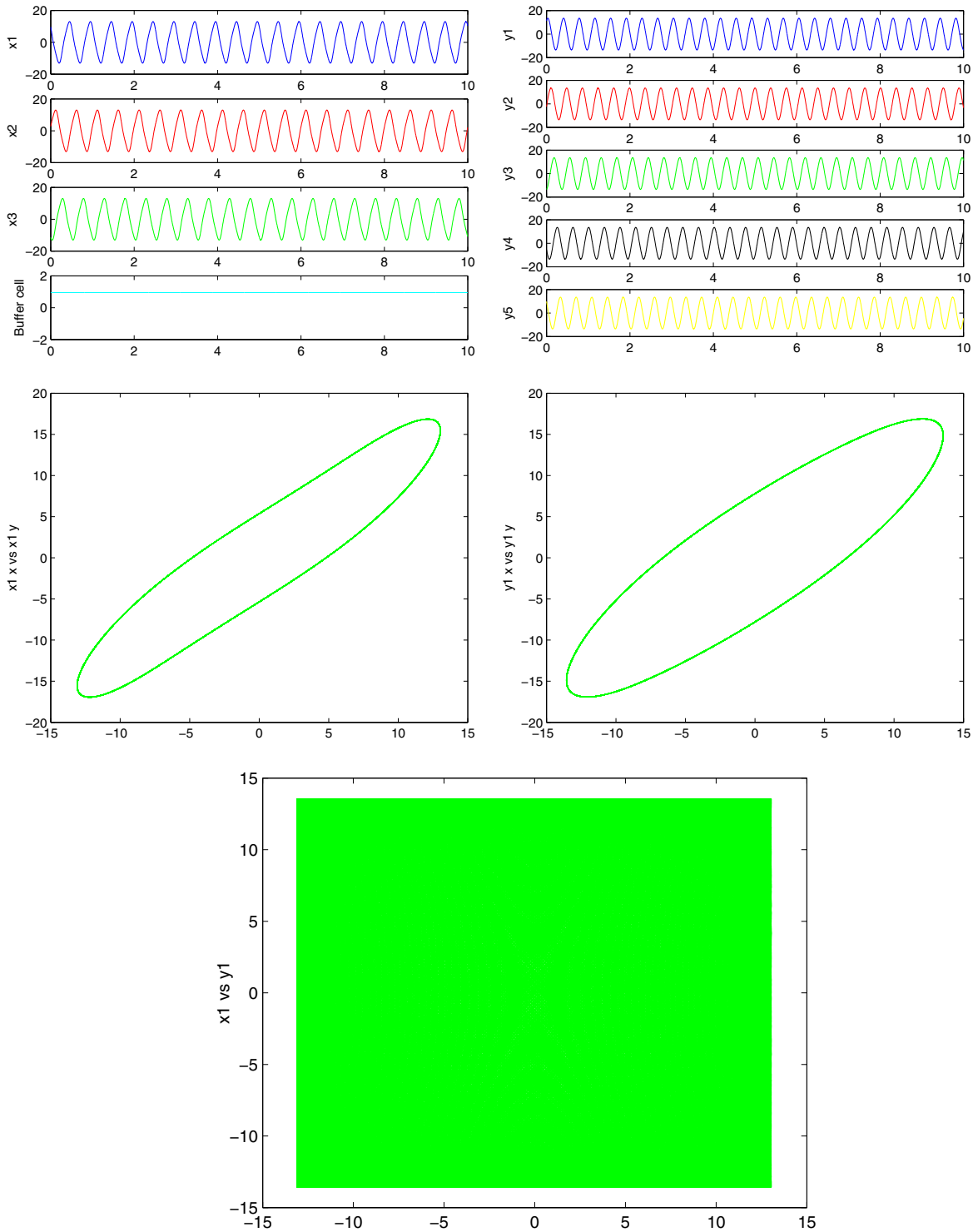

Fig. 10 Simulation of the coupled system (5) with $\mathbf{Z}_3 \times \mathbf{Z}_5$ symmetry, after the seventh Hopf bifurcation point (*HB7*). The cells in the two rings show rotating waves. Phase planes of the oscillator x_1 (*center, left*) and of the oscillator y_1 (*center, right*). Cell x_1 vs cell y_1 (*bottom*). For more information, see text

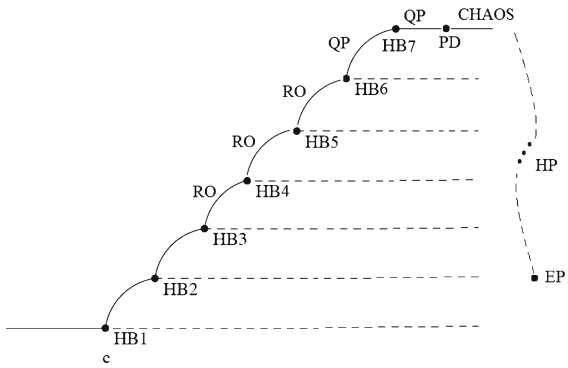

Fig. 11 Schematic (partial) bifurcation diagram for the coupled cell systems considered here, near the equilibrium point. *Solid lines* represent stable solutions, and *dashed lines* correspond to unstable solutions. *HB* Hopf bifurcation, *RO* relaxation oscillation, *QP* quasiperiodic states, *PD* period-doubling bifurcation, *HP* halving-period bifurcation, *EP* end point

$\mathbf{Z}_3 \times \tilde{\mathbf{Z}}_5$ symmetry. The first solution indicates that the primary Hopf bifurcation occured in the 3-ring, leading to a rotating wave in the 3-ring and an equilibrium in the 5-ring. The second type of periodic solution points to a Hopf bifurcation in the 5-ring, leading to a rotating wave in this ring and an equilibrium in the 3-ring.

The secondary branch represented in Fig. 11 is provided by a secondary Hopf bifurcation along the primary branch at the second Hopf bifurcation point (HB2). In the situation where the primary Hopf bifurcation has occurred in the ring 3-ring, we expect that the secondary Hopf bifurcation "occurs" in the remaining ring (the one that displayed equilibrium after the first Hopf bifurcation). On the contrary, if the primary Hopf bifurcation has occured in the 5-ring, the secondary Hopf bifurcation is expected in the 3-ring. The symmetry type of the full solution is $\mathbf{Z}_3 \times \mathbf{Z}_5$ and is quasiperiodic.

The tertiary branch represented in Fig. 11 is provided by a tertiary Hopf bifurcation along the secondary branch at the third Hopf bifurcation point (HB3). In this parameter region, the solution is quasiperiodic with the same symmetry type as in the secondary branch. However, further away along this branch, there is a transition to relaxation oscillation phenomena [22,33].

After the third Hopf bifurcation point, four more Hopf bifurcations take place. We observe that the period and the amplitude of the orbits increases and after the last Hopf point (HB7), the coupled system turns chaotic. It seems like period-doubling bifurcations have taken place, as the parameter c increases. Moreover, increasing a bit more the parameter c, a sequence of halving-period bifurcations seems to take place, and beautiful rotating waves are observed. More work is needed in order to analyze systematically the parameter region, after the seventh Hopf point, and corresponding bifurcations.

Some final comments:

(1) The dynamical behavior of system 5 is much more complex than the one found in [2–4,29], for the same network of two coupled rings with $\mathbf{Z}_3 \times \mathbf{Z}_5$ symmetry, but with simpler internal dynamics for each cell. Thus, the presence of symmetry constrains the dynamical behavior of the cells in each of the rings, but the resonance of the solutions seems to be strongly dependant of the choice of the vector field.

(2) The appearance of relaxation oscillations, after a sequence of Hopf bifurcations, seems to be explained by the network structure. This structure imposes a symmetry group that is a direct product of two symmetry groups, in this case $\mathbf{Z}_3 \times \mathbf{Z}_5$, each of which is a symmetry group of a distinguished sub-network. It is intriguing to observe this type of behavior in these coupled systems since they are not *a priori* multiple time scales systems, where these solutions frequently occur [22,33]. Can these relaxation oscillation phenomena be explained in the context of fast-slow systems through a canard explosion?

(3) The relaxation oscillations in the present study do not produce the curious phenomena, namely the behavior shown in Figs. 9 and 10 of [2], presented first in [15] and studied further in [3], for the $\mathbf{Z}_3 \times \mathbf{Z}_5$ symmetric case. Again, this may depend on the choice of the vector field.

(4) The parameter region to the right of the seventh Hopf bifurcation point produces a huge variety of dynamical phenomena. We believe that closer to (HB7), period-doubling bifurcations take place, and further away halving-period bifurcations appear to "occur." This all happens in a small parameter region. This type of behavior is explained by the properties of the vector field, the Chen oscillator, chosen to model each cell of the two rings.

In Table 1, we summarize the information, computed by XPPAUT, related to the schematic (partial) bifurcation diagram in Fig. 11, and describe the dynamical

Table 1 Summary of the dynamical behavior of coupled cell systems simulated in this work

Branch	c	Symmetry type	3-Ring	5-Ring	Network	Figure
Trivial	15	$\mathbf{Z}_3 \times \mathbf{Z}_5$	Equil.	Equil.	Equil.	
1st (HB1)	15.41	$\mathbf{Z}_3 \times \mathbf{Z}_5$	Equil.	Rot. wave	Periodic	2
2nd (HB2)	15.59	$\mathbf{Z}_3 \times \mathbf{Z}_5$	Rot. wave	Rot. wave	Quasiper.	3
3rd (HB3)	16.29	$\mathbf{Z}_3 \times \mathbf{Z}_5$	Rot. wave	Rel. oscil.	Quasiper.	4
4th (HB4)	18.89	$\mathbf{Z}_3 \times \mathbf{Z}_5$	Rot. wave	Rel. oscil.	Quasiper.	
5th (HB5)	19.54	$\mathbf{Z}_3 \times \mathbf{Z}_5$	Rot. wave	Rel. oscil.	Quasiper.	
6th (HB6)	20.09	$\mathbf{Z}_3 \times \mathbf{Z}_5$	Rot. wave	Quasiper.	Quasiper.	5
7th (HB7)	22.31	$\mathbf{Z}_3 \times \mathbf{Z}_5$	Rot. wave	Chaos	Chaos	6
	22.7	$\mathbf{Z}_3 \times \mathbf{Z}_5$	Quasiper.	Chaos	Chaos	7
	23.5	$\mathbf{Z}_3 \times \mathbf{Z}_5$	Chaos	Rot. wave	Chaos	8
	26.4	$\mathbf{Z}_3 \times \mathbf{Z}_5$	Quasiper.	Rot. wave	Quasiper.	9
	27.6	$\mathbf{Z}_3 \times \mathbf{Z}_5$	Rot. wave	Rot. wave	Quasiper.	10

In the first column, we indicate some branches of solutions with the respective bifurcation points c in column 2. Columns 3–6 show the type of asymptotic stable solutions in the rings and the full systems in the corresponding branch. *equil.* equilibrium, *rot. wave* rotating wave, *rel. oscil.* relaxation oscillation, *quasiper.* quasiperiodic. See text for more details

behavior of the coupled cell systems at the different bifurcating branches.

4 Conclusions

In this paper, we study the dynamical behavior of a network consisting of two rings of chaotic Chen oscillators, which admit $\mathbf{Z}_3 \times \mathbf{Z}_5$ exact symmetry group. We find interesting patterns, some of them explained by local bifurcation theorems and some by the properties of the vector field, the Chen chaotic attractor.

Interesting features like relaxation oscillation, quasiperiod motion, and chaotic states are observed. We compute a partial bifurcation diagram and the corresponding dynamical states in each bifurcating branch. The bifurcation scenario is similar to the one suggested in [15] and [2,3], for the first three Hopf points, and then it is extended to the region where chaos is observed. Period-doubling and halving-period bifurcations seem to take place, providing exciting dynamical features. More work is needed in the future to explain throughly these exotic patterns.

Acknowledgments The author wishes to thank Fundação Gulbenkian, through *Prémio Gulbenkian de Apoio à Investigação 2003*, and the Polytechnic of Porto, through the *PAPRE Programa de Apoio à Publicação em Revistas Científicas de Elevada Qualidade* for financial support. The author was partially funded by the European Regional Development Fund through the program COMPETE and by the Portuguese Government through the FCT—Fundação para a Ciência e a Tecnologia under the project PEst-C/MAT/UI0144/2013. The author thanks the valuable comments from the anonymous reviewers that have very much contributed to the improvement of the quality of the paper.

References

1. Algaba, A., Fernández-Sánchez, F., Merino, M., Rodríguez-Luis, A.J.: Chen's attractor exists if Lorenz repulsor exists: the Chen system is a special case of the Lorenz system. Chaos An Interdiscip. J. Nonlinear Sci. **23**, 033108 (2013)
2. Antoneli, F., Dias, A.P.S., Pinto, C.M.A.: Quasi-periodic states in coupled rings of cells. Commun. Nonlinear Sci. Numer. Simul. **15**(15), 1048–1062 (2010)
3. Antoneli, F., Dias, A.P.S., Pinto, C.M.A.: Rich phenomena in a network of two ring coupled through a 'buffer' cell. In: Proceedings of the 2nd Conference on Nonlinear Science and Complexity NSC2008 (2008)
4. Antoneli, F., Dias, A.P.S., Pinto, C.M.A.: New phenomena in coupled rings of cells. In: Proceedings of the 3rd IFAC Workshop on Fractional Differentiation and its Applications FDA2008 (2008)
5. Ashwin, P., Buescu, J., Stewart, I.: Bubbling of attractors and synchronisation of oscillators. Phys. Lett. A **193**, 126–139 (1994)
6. Ashwin, P., Burylko, O., Maistrenko, Y.: Bifurcation to heteroclinic cycles and sensitivity in three and four coupled phase oscillators. Phys. D **237**(4), 454–466 (2008)
7. Bressloff, P.C., Cowan, J.D., Golubitsky, M., Thomas, P.J.: Scalar and pseudoscalar bifurcations: pattern formation in the visual cortex. Nonlinearity **14**, 739–775 (2001)
8. Buono, P.-L.: Models of central pattern generators for quadruped locomotion: II. Secondary gaits. J. Math. Biol. **42**(4), 327–346 (2001)

9. Buono, P.-L., Golubitsky, M.: Models of central pattern generators for quadruped locomotion: I. Primary gaits. J. Math. Biol. **42**(4), 291–326 (2001)
10. Cohen, J., Stewart, I.: Polymorphism viewed as phenotypic symmetry-breaking. In: Malik, S.K. (ed.) Nonlinear Phenomena in Physical and Biological Sciences, pp. 1–67. Indian National Science Academy, New Delhi (2000)
11. Collins, J.J., Stewart, I.: Coupled nonlinear oscillators and the symmetries of animal gaits. J. Nonlinear Sci. **3**, 349–392 (1993)
12. Chen, G., Ueta, T.: Yet another chaotic attractor. Int. J. Bifurcation Chaos **9**, 1465–1466 (1999)
13. Ermentrout, B.: XPPAUT®—the differential equations tool, version 5.98. http://www.math.pitt.edu/bard/xpp/xpp.html (2006)
14. Filipski, N., Golubitsky, M.: The Abelian Hopf H mod K theorem. SIAM J. Appl. Dyn. Syst. **9**(2), 283–291 (2010)
15. Golubitsky, M., Nicol, M., Stewart, I.: Some curious phenomena in coupled cell systems. J. Nonlinear Sci. **14**, 207–236 (2004)
16. Golubitsky, M., Stewart, I.: Nonlinear dynamics of networks: the groupoid formalism. Bull. Am. Math. Soc. **43**, 305–364 (2006)
17. Golubitsky, M., Stewart, I.: The Symmetry Perspective: From Equilibrium to Chaos in Phase Space and Physical Space. Progress in Mathematics, vol. 200. Birkhäuser, Basel (2002)
18. Golubitsky, M., Stewart, I., Török, A.: Patterns of synchrony in coupled cell networks with multiple arrows. SIAM J. Appl. Dyn. Syst. **4**(1), 78–100 (2005)
19. Golubitsky, M., Stewart, I., Schaeffer, D.G.: Singularities and Groups in Bifurcation Theory, vol. 2. Applied Mathematical Sciences 69. Springer-Verlag, New York (1988)
20. Gu, H.: Experimental observation of transition from chaotic bursting to chaotic spiking in a neural pacemaker. Chaos **23**, 023126 (2013)
21. Jiang, B., Han, X., Bi, Q.: Hopf bifurcation analysis in the T system. Nonlinear Anal. **11**, 522–527 (2010)
22. Krupa, M., Szmolyan, P.: Relaxation oscillations and canard explosion. J. Differ. Equ. **174**, 312–368 (2001)
23. Kuramoto, Y.: Chemical Oscillations, Waves, and Turbulence. Springer, Berlin (1984)
24. Labouriau, I.S., Alves-Pinto, C.M.: Loss of synchronization in partially coupled Hodgkin–Huxley equations. Bull. Math. Biol. **66**, 539–557 (2004)
25. Lü, J.H., Zhou, T.S., Chen, G.R., Zhang, S.C.: Local bifurcation of the Chen system. Int. J. Bifurcation Chaos **12**, 2257–2270 (2002)
26. Nguimdo, R.M., Tchitnga, R., Woafo, P.: Dynamics of coupled simplest chaotic two-component electronic circuits and its potential application to random bit generation. Chaos **23**, 043122 (2013)
27. Pecora, L.M., Carroll, T.L.: Synchronization in chaotic systems. Phys. Rev. Lett. **64**, 821–824 (1990)
28. Pinto, C.M.A.: Stability of quadruped robots' trajectories subjected to discrete perturbations. Nonlinear Dyn. **70**, 2089–2094 (2012)
29. Pinto, C.M.A.: Exotic dynamics in networks of coupled rings of cells. Int. J. Bifurcation Chaos **22**(3), 1250064 (2012)
30. Pinto, C.M.A., Golubitsky, M.: Central pattern generators for bipedal locomotion. J. Math. Biol. **53**(3), 474–489 (2006)
31. Santos, C.P., Matos, V., Pinto, C.M.A.: A Brainstem-like modulation approach for gait transition in a quadruped robot. In: Proceeding of the 2009 IEEE/RSJ International Conference on Intelligent RObots and Systems, IROS 2009 (2009)
32. Stewart, I., Golubitsky, M., Pivato, M.: Symmetry groupoids and patterns of synchrony in coupled cell networks. SIAM J. Appl. Dyn. Syst. **2**(4), 609–646 (2003)
33. Szmolyan, P., Wechselberger, M.: Canards in $\mathbf{R}^3$. J. Differ. Equ. **177**, 419–453 (2001)
34. The MathWorks, Inc. MATLAB®, 1994–2012. http://www.mathworks.com